

# Numerical modeling of wave-current interaction in Merak Port, Indonesia

**S Nurfitri, N S Ningsih, A N Sentanu and R Rachmayani**

Department of Oceanography, Bandung Institute of Technology, Jalan Ganesha 10, Bandung 40132, Indonesia

E-mail: suliskania.n@oceanography.itb.ac.id

**Abstract.** This study aimed to investigate the effects of currents to wave height in the waters of Merak Port, Banten using wave spectrum model. The wave-current interaction simulation was performed by utilizing SWAN (Simulating Waves Nearshore) in stationary mode and using the unstructured triangular grid. Data of wind velocity and direction as model inputs were obtained from BMKG (Indonesian Agency for Meteorology, Climatology, and Geophysics), whereas tidal current velocity data was obtained from TMD (Tide Model Driver). The model was simulated in two different scenarios, i.e. without and with following (adverse) current which is same (opposite) with wave propagation. The model input of dominant west wind was used to represent the west monsoon, while the dominant wind from the north was used to represent the east monsoon. The simulation results show that the maximum wave height is 2.98 m in the west monsoon and 1.9 m in east monsoon. In the west (east) monsoon the following current decrease wave height to 9.26% (5.09%), while the adverse current increase wave height up to 9.07% (6.56%).

## 1. Introduction

Merak Port, Cilegon, Banten is the port which devoted ship transportation from Java Island to Sumatra and vice versa. The water transportation activity at this port is highly depends on the wave condition. Wave height is one of the major factors which affects the ship performance and safety [1]. Wave condition is strongly influenced by wind variability which is the main generating force (dominant) of sea wave [2, 3]. Ocean circulation of Indonesian sea, here in particular, Java Sea is affected by the monsoon cycle. From December to March the wind blows southeastward and eastward near the equator [4]. It is known as the northwest monsoon or in Java it is also called west monsoon. On the contrary, from June to September, the prevailing wind blows northwestward from Australia [4]. In Java Sea, the wind blows from the east, thus it is called east monsoon.

The previous study of ocean waves in Sunda Strait area using SWAN (Simulating Waves Nearshore) spectrum model has been conducted by Ramadhan (2014) and Adiprabowo (2015) [2, 5]. Adiprabowo (2015) conducted two stages of nested modeling using a regional model by Ramadhan (2014) as a large model with non-stationary and stationary mode [5]. The simulation was using the dominant wind field at Serang Station during 2003-2013. The result shows that the maximum wave height ( $H_{max}$ ) at southern Sunda Strait in west monsoon is 3.2 m and east monsoon is 1.6 m [5].

Study of wave-current interaction has been conducted by Baddour and Song (1990) and Wolf and Prandle (1999). Waves which propagate in the area of current circulation may experience the changes of wave height and wavelength [6, 7]. When the waves propagate in the same direction with current, significant wave height decreased and wavelength increased. Meanwhile, when the wave propagates in



the opposite direction with current, wave height increased and wavelength decreased [6, 7, 8]. The previous study of wave-current interaction also conducted by Hein et al (2011) using SWAN coupled with HAMSOM in Ems-Dollard Estuary [9]. Generally, the results show that in shallow regions the difference between the simulation of waves, with and without currents is less than 10% [9]. On the other hand, inside tidal channels, the difference can exceed 25% [9].

This study aimed to investigate the effects of currents to wave height in the waters of Merak Port, Banten, Sunda Strait using wave spectrum model. The interaction of wave and current can produce extreme wave height which caused the disruption of ship transportation and also ship docking at the port. The research was conducted by utilizing SWAN. The scope of research is covering the Sunda Strait, here in particular Merak Port. Constant wind velocity (spatial and temporal) which used as generating force. In addition to that, the tidal current was taking into account.

## 2. Methodology

### 2.1. Wave equations

SWAN is based on the Eulerian formulation of the discrete spectral balance of action density that accounts for refractive propagation over arbitrary bathymetry and current fields [10]. SWAN solves the evolution of the wave spectrum by using the action density spectrum [8]. In the presence of ambient current, the action density is conserved while the energy density is not [8]. The action density  $N(\sigma; \theta)$  is equal to the energy density  $E(\sigma; \theta)$  divided by the relative angular frequency  $\sigma$ , i.e.  $N(\sigma; \theta) = E(\sigma; \theta)/\sigma$ . SWAN solves the evolution of the wave spectrum by using the action density spectrum [8]. The governing equation for Cartesian coordinates is [8, 11]:

$$N(\sigma, \theta) = \frac{E(\omega, \theta)}{\sigma} \quad (1)$$

$$\frac{\partial}{\partial t} N + \frac{\partial}{\partial x} c_x N + \frac{\partial}{\partial y} c_y N + \frac{\partial}{\partial \sigma} c_\sigma N + \frac{\partial}{\partial \theta} c_\theta N = \frac{S_{tot}}{\sigma} \quad (2)$$

where  $x$  and  $y$  are horizontal Cartesian coordinates,  $t$  is time,  $\theta$  is the propagation direction of each wave component,  $c_x$ ,  $c_y$ ,  $c_\sigma$ , and  $c_\theta$  are the propagation velocity in  $x$ -space,  $y$ -space,  $\sigma$ -space, and  $\theta$ -space respectively [8].  $S$  is the source term in terms of energy density, which include the effects of generation, dissipation, and nonlinear wave-wave interaction [8]. The first term on the left-hand side of equation (2) is the rate of change of action density in time, the second and third terms are the propagation of action in physical space [8]. The fourth and fifth terms show the shifting of the relative frequency and the refraction due to variations in depth and currents [8].

### 2.2. Model domain and parameters

Area of interest of the study is covering Java Sea, Sunda Strait, and Indian Ocean (figure 2) and focused on Merak Port (figure 2). Model inputs are dominant wind velocity, bathymetry, coastline and current velocity. Wind data obtained from BMKG (Indonesian Agency for Meteorology, Climatology, and Geophysics). Bathymetry data obtained from GEBCO (Global Bathymetric Chart of Oceans) resolution 30" and coastline from GSHHG (Global Self-consistent, Hierarchical, High-Resolution Geography Database) [12, 13]. Meanwhile, current velocity obtained from TMD (Tide Model Driver) [14].

The wave simulation utilized unstructured triangular grid as shown in figure 1 which generated by mesh generator MESH2D. Physical processes during the wave simulation are wave generation, quadruplet nonlinear interaction, dissipation and current-wave interaction. The boundary condition is the open boundary. There are 6 model scenarios which showed in Table 1. The scenarios are divided based on wind and current direction (table 1). The current is divided into two directions i.e. following (FC) and adverse current (AC) which has the same and opposite direction with wave propagation.

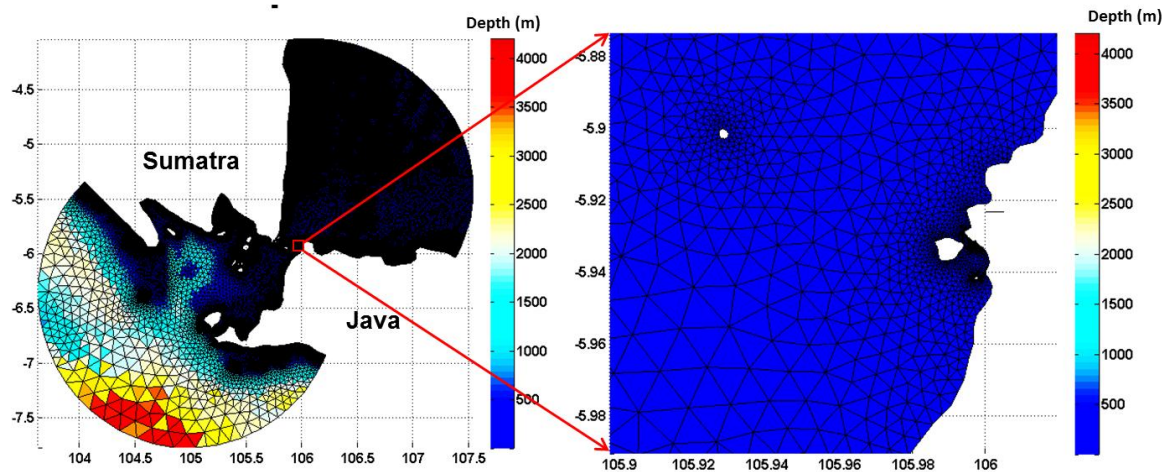


**Figure 1.** Model grid

**Table 1.** Model scenarios

Sc.	Wind velocity (from-)	Current
1	West (10.28 m/s)	No Current
2	North (7.72 m/s)	No Current
3	West (10.28 m/s)	Following Current (FC)
4	North (7.72 m/s)	Adverse Current (AC)
5	West (10.28 m/s)	Adverse Current (AC)
6	North (7.72 m/s)	Following Current (FC)

### 3. Results and discussion

#### 3.1. Model verification

The model verification was done by compared the  $H_s$  (significant wave height) with reference model by Adiprabowo (2015) at 3 locations (figure 2). Wave simulation using west wind as generating force representation of west monsoon, meanwhile east monsoon represents the north wind. Generally, wave propagation is agreed with the wind direction. For example, the west wind generates eastward wave and north wind generates the southward wave.

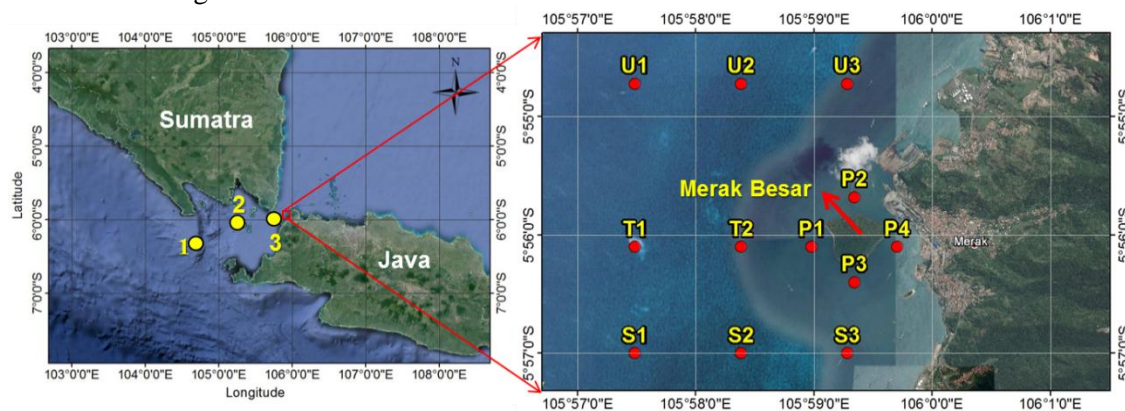


**Figure 2.** Area of interest (right). Location of model verification show by the yellow circles (left).

**Table 2.** Model verification results

St.	Adiprabowo (2015)				This study			
	West monsoon		East monsoon		West monsoon		East monsoon	
	$H_s$ (m)	$H_{max}$ (m)	$H_s$ (m)	$H_{max}$ (m)	$H_s$ (m)	$H_{max}$ (m)	$H_s$ (m)	$H_{max}$ (m)
1	1.6	3.2	0.8	1.6	1.5	3.0	0.8	1.6
2	1.5	3.0	0.6	1.2	1.5	3.0	0.7	1.4
3	1.2	2.4	0.5	1.0	1.4	2.8	0.7	1.4
Bias (m)					0.03		0.01	
RMSD (m)					0.13		0.13	
CC					0.97		0.94	

Significant wave height in west monsoon is higher than east monsoon. It is caused by the dominant wind velocity is faster than east monsoon. The results agree with verification results conducted by Adiprabowo (2015) in Sunda Strait [5]. The model verification produce the bias 0.03 m in west monsoon and 0.01 m in east monsoon (table 2). These results show that the model overestimates compared to referenced model by Adiprabowo (2015). In addition to that, the RMSD (Root Mean Square Difference) is 0.13 both in west and east monsoon. Meanwhile, the coefficient correlation is relatively high, that is 0.97 and 0.94 in west and east monsoon.

### 3.2. Wave-current interaction

There are two different of current direction which used in this research i.e. following and adverse current. Following current (FC) was used when the current direction is same with wave propagation. While adverse current (AC) was used if the current direction is opposite with wave propagation. The vector of current and wind which generated wave is shown in figure 3. Scenario 3 represented the west monsoon when flood tide, hence the current is in the same direction with wave propagation (FC). Meanwhile, scenario 5 represent the ebb tide, so that the current direction is opposite with wave propagation (AC). Scenario 4 represented the east monsoon when flood tide, hence the current is opposite with wave propagation (AC). While scenario 6 represented the ebb tide so that the current is in the same direction with wave propagation (FC).

Figure 4 shows the  $H_s$  differences between three scenarios in west monsoon. The percentage of  $H_s$  difference between a simulation with and without current in the west monsoon is -9.26% (FC) and +9.07% (AC). Meanwhile in east monsoon,  $H_s$  alteration is -5.09% (FC) and +6.56% (AC). Negative (positive) sign show the decreasing (increasing) of  $H_s$ . These simulation results show that the current direction affects the significant wave height ( $H_s$ ). When the wave propagates in the same direction with current, significant wave height decreased. Meanwhile, when the wave propagates in the opposite direction with current,  $H_s$  increased.

The condition which affects the port activities and ship transportation significantly is when the wave propagating in the opposite direction with the current. In this experiment, the adverse current occurs when ebb tide (flood tide) in west monsoon (east monsoon) as shown in scenario 5 (scenario 4). Both in west and east monsoon,  $H_s$  increment is below 10%. Despite the relatively small percentage, the  $H_s$  increment may affect the ship transportation, especially if the  $H_s$  with no current effects is equal or more than 2 meters. As stated on 'Guide the Marine Meteorological Services, Third Edition' that almost all the sailing ship will be disrupted by the wave which has  $H_s \geq 2$  meters [15].



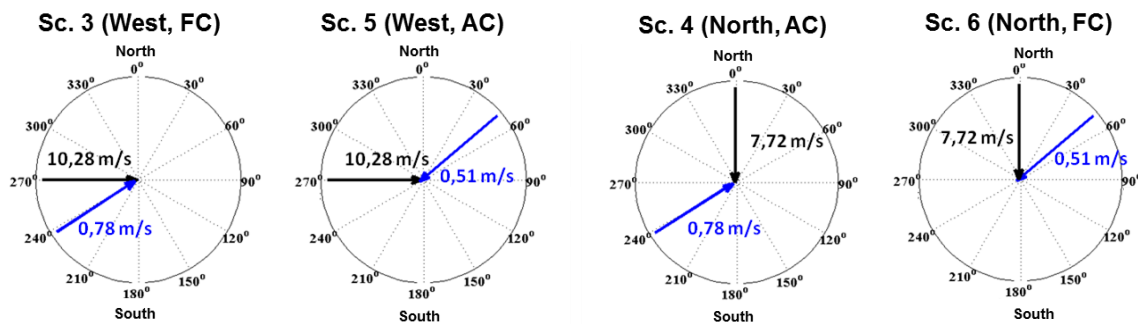


**Figure 3.** Wind (black) and current (blue) direction.

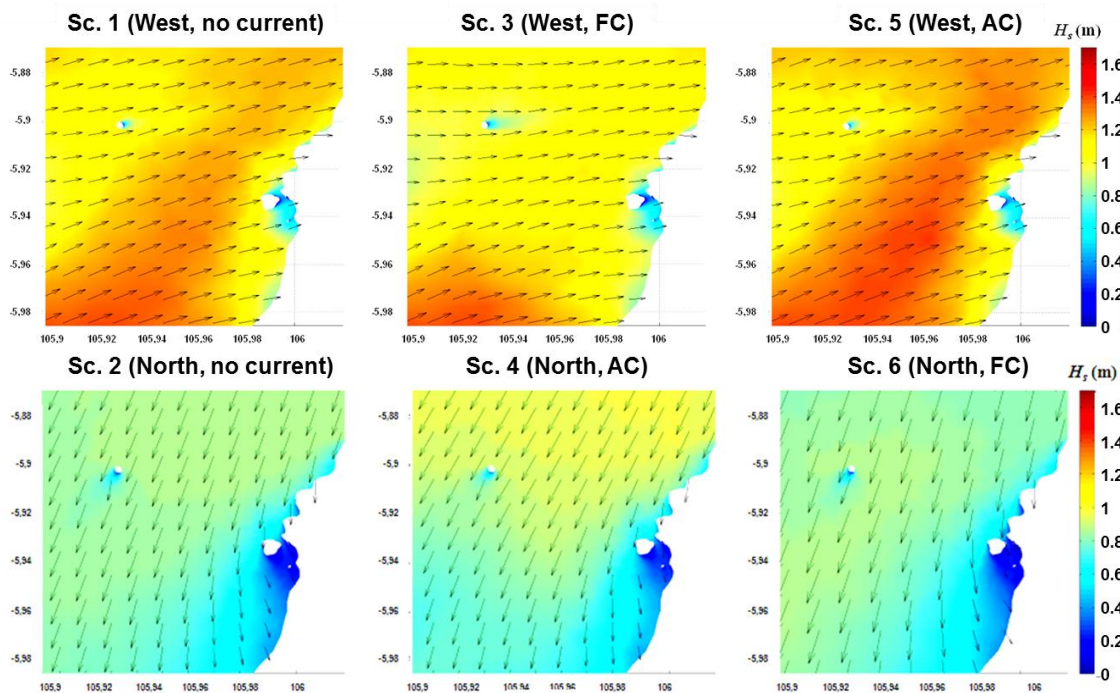


**Figure 4.** The significant wave height in the west monsoon (above) and the east monsoon (below). The vector arrows show the direction of wave propagation.

The graph in figure 5 and figure 6 show the comparison of energy spectrum in several points. The graph represents energy change during wave propagation from the open sea to shore. Generally, the energy density spectrum of the wave with adverse current is larger than without current, whereas the smallest is the following current. In the west monsoon, the energy spectrum from open sea (T1) to nearshore (P1) is decreasing (figure 5). The  $H_s$  reduction is up to 0.18 m. This happened because of energy dissipation due to shallower waters. Energy density is decreasing in P4 because this area is being covered by Merak Besar Island. The  $H_s$  reduction in P4 is 0.58 m which is higher than P1.

In east monsoon which the wave propagates from the north, the energy density is decreasing from U3 to P2 and P3, then increasing in S3 (figure 6). Point P3 (behind Merak Besar Island) is the 'covered' area, so it has lower energy than in P2 (in front of Merak Besar Island). Even S3 also located behind Merak Besar Island, but its location is further than P3. It causes S3 has longer fetch (wave generating area) and generates higher  $H_s$  than P3 (figure 6).

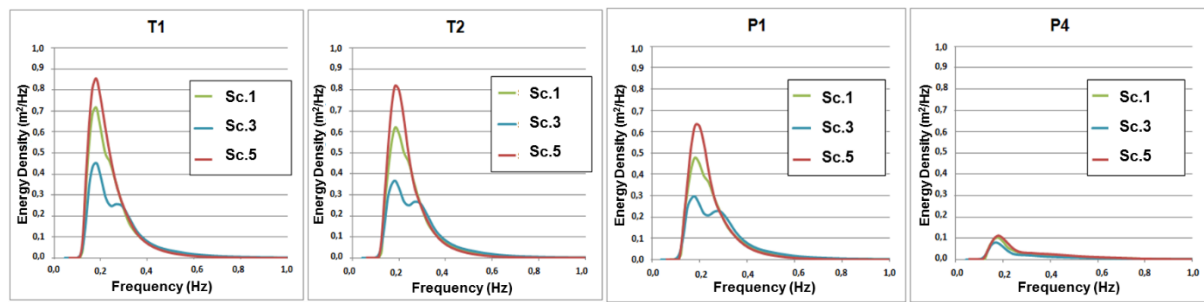


**Figure 5.** The energy density spectrum 1 dimension during the west monsoon.

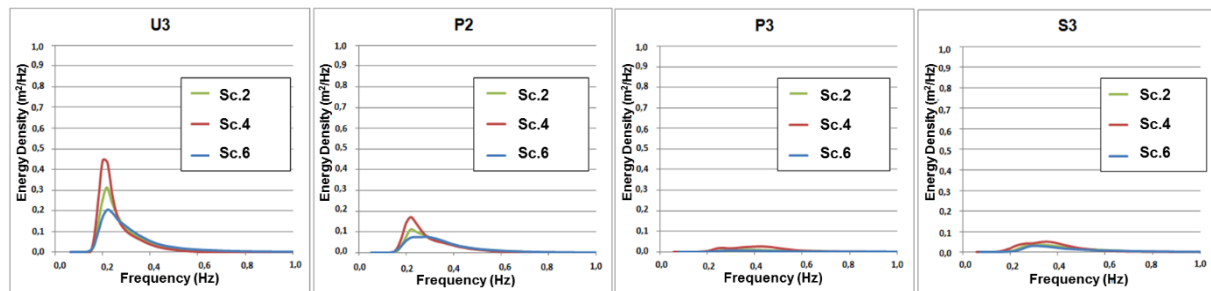


**Figure 6.** The energy density spectrum 1 dimension during the east monsoon.

The energy density of wave in west monsoon is higher than east monsoon. It caused by the wind velocity in west monsoon (10.28 m/s) is higher than east monsoon (7.72 m/s). The graph (figure 5 and figure 6) show that energy density of wave which propagates along with adverse current as scenario 4 and 5 has the highest value among other scenarios. In the contrary, the energy density of wave which propagates along with following current as scenario 3 and 6 has lower value compared to no current simulation as scenario 1 and 2.

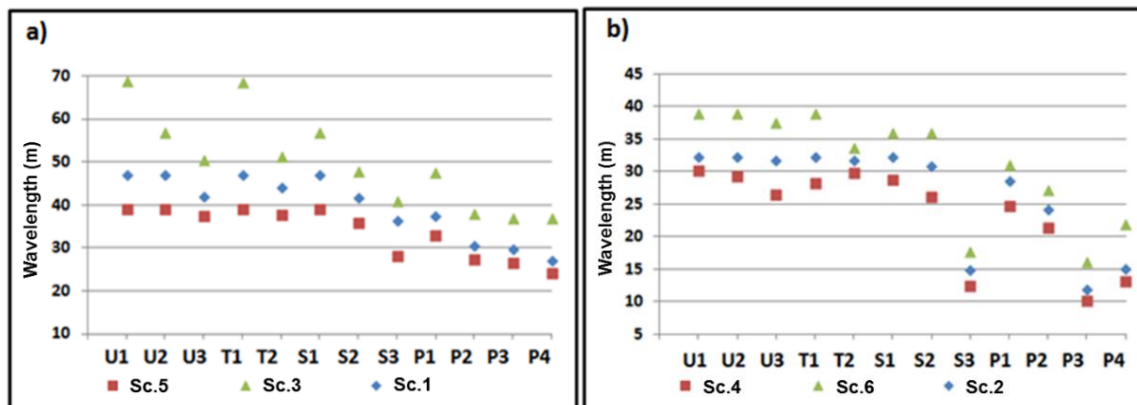


**Figure 7.** Wavelength calculated by Fenton equation in a) west; b) east monsoon.

The wavelength was calculated using the dispersive wave equation by Fenton (1988) [16, 17]. Based on that calculation, the wave which propagates along with adverse current has a shorter wavelength than following current (figure 7). The shorter wavelength correlate with higher wave height and vice versa. The correlation between wavelength and wave height is associated with the law of continuity or conservation of mass during the wave propagation. When the wave encounters the current in opposite direction, the water mass is accumulated and caused the wave height increase. As the result, the wavelength is decreasing.

#### 4. Conclusions

Simulation of wave propagation with the following current produced  $H_{max}$  (maximum wave height) in west and east monsoon by 2.27 m and 1.56 m. Furthermore, the simulation with adverse current produced the higher  $H_{max}$  i.e. 2.98 m in the west and 1.90 m in the east monsoon. The following current decreased wave height by 9.26% in the west and 5.09% in the east monsoon. On the contrary, the adverse current increased  $H_{max}$  by 9.07% in the west and 6.56% in the east monsoon.

#### References

- [1] Cai Y, Wen Y and Wu L 2014 Ship route design for avoiding heavy weather and sea conditions *J. Mar. Navig. Saf. Sea Transport.* **8** 551-556
- [2] Arinaga R A and Cheung K F 2012 Atlas of global wave energy from 10 years of reanalysis and hindcast *Renew. Energ.* **39** 49-64
- [3] Ramadhan H 2014 *Characteristics and Analysis of Waves in West Indonesian Waters using Wave Spectrum Model* (Indonesia: ITB)
- [4] Putri M R 2005 *Study of Ocean Climate Variability (1959-2002) in the Eastern Indian Ocean, Java Sea and Sunda Strait Using the HAMburg Shelf Ocean Model* (Germany: University of Hamburg)
- [5] Adiprabowo S 2015 *Study of Wave Characteristics in Sunda Strait using Wave Spectrum Model* (Indonesia: ITB)
- [6] Baddour R E and Song S 1990 On the Interaction between Waves and Currents *Ocean Eng.* **17** 1-21
- [7] Wolf J and Prandle D 1999 Some Observation of Wave-Current Interaction *Coast. Eng.* **37** 471-485
- [8] Qin W, Kirby J T and Badiy M 2005 Application of the spectral wave model SWAN in Delaware Bay *Res. Rep.* (Newark: Center for Applied Coastal Research)
- [9] Hein H, Mai S and Barjenbruch U 2011 Interaction of wind-waves and currents in the Ems-Dollard Estuary *Int. J. Ocean Clim.* **2** 249-258
- [10] Booij N, Ris R C and Holthuijsen L H 1999 A third-generation wave model for coastal regions 1. Model description and validation *J. Geophys. Res.* **104** 7649-7666
- [11] Tolman H L 1988 Propagation of wind waves on tides *Coast. Eng.* 512-523
- [12] OC, IHO, and BODC 2003 *Centenary Edition of the GEBCO Digital Atlas* (Liverpool: British Oceanographic Data Centre)
- [13] Wessel P and Smith W H F 1996 A Global Self-consistent, Hierarchical, High-resolution Geography Database *J. Geophys. Res.* **101** 8741-8743
- [14] Padman L and Erofeeva S 2005 *Tide Model Driver (TMD) Manual* (Seattle: Earth & Space Research)
- [15] World Meteorological Organization (WMO) 2001 *Guide the marine meteorological services, Third Edition* (Geneva: Author)
- [16] Holthuijsen L H 2007 *Wave in ocean and coastal waters* (New York: Cambridge)
- [17] Fenton J D 1988 The numerical solution of steady water wave problems *Comput. Geosci.* **14** 357-368